

# An adaptive inverse control method based on SVM–fuzzy rules acquisition system for pulsed GTAW process

Xixia Huang · Wei Gu · Fanhuai Shi · Shanben Chen

Received: 4 March 2008 / Accepted: 2 December 2008 / Published online: 9 January 2009  
© Springer-Verlag London Limited 2008

**Abstract** This paper proposes a new method of adaptive inverse control based on support vector machine–fuzzy rules acquisition system (SVM-FRAS) for the gas tungsten arc welding (GTAW) process. In this control mechanism, an identifier is established based on SVM-FRAS, and an inverse controller based on SVM-FRAS is designed. The proposed adaptive inverse control method can automatically extract control rules from the process data. Comprehensibility is one of the required characteristics for a complex GTAW process control. We use the proposed SVM-FRAS-based adaptive inverse control method to obtain the rule-based process and the control model of the aluminum alloy pulse GTAW process. Based on the simulation experiments for GTAW process, the SVM-FRAS adaptive inverse control method is found to be effective.

**Keywords** Adaptive inverse control · Support vector machine · Fuzzy rule · Arc welding

## 1 Introduction

Control engineers and weld technologists are often confronted by problems such as controlling the weld quality

like welding penetration and the fine formation of the welding bead. To obtain the fine formation of the weld seam, the sizes of weld pool should be exactly dominated in real time, that is, the backside and topside width. In addition, the control of the weld pool shape is a critical issue in automated as well as robotic welding. However, modeling and control for this process by classical methods are difficult to realize. There are mainly two kinds of reasons. Firstly, the arc welding process is characterized as inherently nonlinear, bound to time-delay, and has strong coupling in its input/output relationships as it involves a number of uncertain factors such as metallurgy, heat transfer, chemical reaction, arc physics, and magnetization. Another reason is that not only accuracy but also comprehensibility should be considered when modeling and control in the welding process. In general, comprehensibility is one of the required characteristics of reliable systems, especially in complex welding processes, which are affected by various factors. Therefore, a model with poor comprehensibility is deemed to be unreliable. It is still very difficult to obtain a model that is comprehensible and simultaneously has satisfactory generalization capability.

Recent decade, several approaches using artificial intelligence have been proposed to model and control for the arc welding process, such as the neural network (NN) [1, 2], fuzzy set (FS) [3], and rough set (RS) [4, 5]. Some studies have evidently shown the efficiency of the above-mentioned methods in obtaining the model of the arc welding process under certain conditions. However, NN is a “black box”, which means that with this method, the model becomes impossible to directly read and modify. On the other hand, the conventional FS method directly depends on the experience of the human operator, which is actually difficult to obtain. Moreover, the number of inputs, outputs, and their linguistic variables could not be too large;

X. Huang (✉) · W. Gu  
Marine Technology & Control Engineering Key Laboratory,  
Shanghai Maritime University,  
1550 Pudong Ave.,  
Shanghai 200135, China  
e-mail: merryhuang1975@gmail.com

F. Shi · S. Chen  
Welding Engineering Institute, School of Materials Science and  
Engineering, Shanghai Jiao Tong University,  
800 Dongchuan Road,  
Shanghai 200240, China

otherwise, this will lead to “rule explosion”. With respect to the RS method, the task of prediction is not very effective, and hence, it is more like a tool for data description. In view of these difficulties, it is then necessary to develop more practical modeling methods for complex welding processes.

Support vector machine (SVM), developed by Vapnik [6, 7], is gaining popularity due to its various attractive features and promising empirical performance. Originally, SVM is developed for pattern recognition problems, but in recent years, with the introduction of  $\varepsilon$ -insensitive loss function, SVM has been extended to solve nonlinear regression estimation, time-series prediction, system nonlinear identification, and control.

Recently, Huang and Chen [8] have proposed a fuzzy modeling method based on SVM for the arc welding process. In [8], SVM is used to extract IF–THEN rules; the fuzzy basis function inference system is adopted as the fuzzy inference system. So the approach possesses good comprehensibility as well as satisfactory generalization capability. Based on [8], we introduce a new support vector machine–fuzzy rules acquisition system (SVM-FRAS). In SVM-FRAS, we apply adaptive learning to tune the fuzzy rules and parameters in the fuzzy inference system automatically. Based on the previous modeling work, we apply SVM-FRAS to welding process control in this paper. A new adaptive inverse control method based on SVM-FRAS is proposed for the GTAW process. In this control mechanism, an identifier is established based on SVM-FRAS, and an inverse controller based on SVM-FRAS is designed. Finally, the simulation experiment on the arc welding process is also conducted.

## 2 Preliminaries of the fuzzy basis function inference system and SVM for regression

This section of the paper provides background knowledge about the fuzzy basis functions [9] and SVM for regression [10] for the convenience of the readers.

### 2.1 Fuzzy basis function inference system

The most common fuzzy rule-based system consists of a set of linguistic rules in the following form:

IF premise (antecedent)  
THEN conclusion (consequent)

This form is referred to as the IF–THEN rule. It typically expresses an inference, such that if we know the fact (premise), then we can infer another fact (conclusion). In this study, the general case where the fuzzy rule base

consists of  $M$  rules is considered and is in the following form:

$R_j$  : IF  $x_1$  is  $A_1^j$  and  $x_2$  is  $A_2^j$  and ... and  $x_n$  is  $A_n^j$ ,  
THEN  $z$  is  $B^j$  for  $j = 1, 2, \dots, M$

where  $R_j$  is the fuzzy rule,  $x_i(i=1,2,\dots,n)$  are the input variables,  $z$  is the output variable of the fuzzy system, and  $A_i^j$  and  $B^j$  are the linguistic terms characterized by fuzzy membership function  $u_{A_i^j}(x_i)$  and  $u_{B^j}(z)$ , respectively.

The overall fuzzy inference function is

$$f(x) = \frac{\sum_{j=1}^M \bar{z}^j \left( \prod_{i=1}^n u_{A_i^j}(x_i) \right)}{\sum_{j=1}^M \left( \prod_{i=1}^n u_{A_i^j}(x_i) \right)} \tag{1}$$

where  $f:R^n \rightarrow R$ ,  $u_{A_i^j}(x_i)$  is the Gaussian membership function, and  $\bar{z}^j$  is the point in the output space at which  $u_{B^j}(z)$  achieve its maximum value.

In this case, the fuzzy basis function can be denoted as

$$p_j(x) = \frac{\prod_{i=1}^n u_{A_i^j}(x_i)}{\sum_{j=1}^M \left( \prod_{i=1}^n u_{A_i^j}(x_i) \right)}. \tag{2}$$

Then  $f(x)$  can be viewed as a linear combination of the fuzzy basis function (FBF). In other words, the fuzzy inference system in Eq. 1 is equivalent to the FBF expansion

$$f(x) = \sum_{j=1}^M p_j(x) \bar{z}^j. \tag{3}$$

Moreover, this linear combination of fuzzy basis function is capable of evenly approximating any real continuous function on a compact set to arbitrary accuracy.

### 2.2 SVM for regression estimation

We further describe the linear function using the form  $\langle \varpi \cdot x \rangle + b$ . As to the nonlinear case, we transfer the nonlinear problem into a linear problem using a nonlinear map  $\varphi(x)$  from the low dimensional input space to a higher-dimensional feature space. SVM approximates the function using the following form:

$$f(x) = \langle \varpi \cdot \phi(x) \rangle + b. \tag{4}$$

The regression problem is equivalent to the following optimization problem:

$$\begin{aligned} \min \quad & \frac{1}{2} \|\varpi\|^2 + C \sum_{i=1}^l (\xi_i + \xi_i^*) \\ \text{s.t.} \quad & \begin{cases} y_i - \langle \varpi^T \cdot \phi(x_i) \rangle - b \leq \varepsilon + \xi_i \\ \langle \varpi^T \cdot \phi(x_i) \rangle + b - y_i \leq \varepsilon + \xi_i^* \\ \xi_i, \xi_i^* \geq 0 \end{cases} \end{aligned} \tag{5}$$

where minimizing  $\|\varpi\|^2/2$  means minimizing the model’s complexity and, at the same time,  $f(x)$  approximately pairs  $(x_i, y_i)$  with  $\varepsilon$  precision. Thus, the above optimization problem is a realization of the structure risk minimization principle. Therefore, the obtained regression estimation possesses reliable generalization ability.  $C>0$  is cost coefficient, which represents a balance between the model’s complexity and the approximation error. When the constraint conditions are unfeasible, slack variables  $\xi_i, \xi_i^*$  should be introduced.

To solve the optimization problem more easily, dual formulation is obtained by utilizing Lagrange multipliers:

$$\begin{aligned} \min_{\alpha, \alpha^*} \quad & \frac{1}{2} (\alpha - \alpha^*)^T Q (\alpha - \alpha^*) + \varepsilon \sum_{i=1}^l (\alpha_i + \alpha_i^*) + \sum_{i=1}^l y_i (\alpha_i - \alpha_i^*) \\ \text{s. t.} \quad & \sum_{i=1}^l (\alpha_i - \alpha_i^*) = 0, 0 \leq \alpha_i, \alpha_i^* \leq C, i = 1, \dots, l, \end{aligned} \tag{6}$$

where  $Q_{ij} = K(x_i, x_j) \equiv \phi(x_i)^T \phi(x_j)$  is the so-called kernel function.

Based on the Karush–Kuhn–Tucker conditions [11, 12], the samples can be classified into:

- $E$  set: error support vectors:  $E = \{i \mid |\alpha_i - \alpha_i^*| = C\}$
- $S$  set: margin support vectors:  $S = \{i \mid 0 < |\alpha_i - \alpha_i^*| < C\}$
- $R$  set: remaining samples:  $R = \{i \mid \alpha_i - \alpha_i^* = 0\}$

By solving Eq. 6, the approximate function is then obtained:

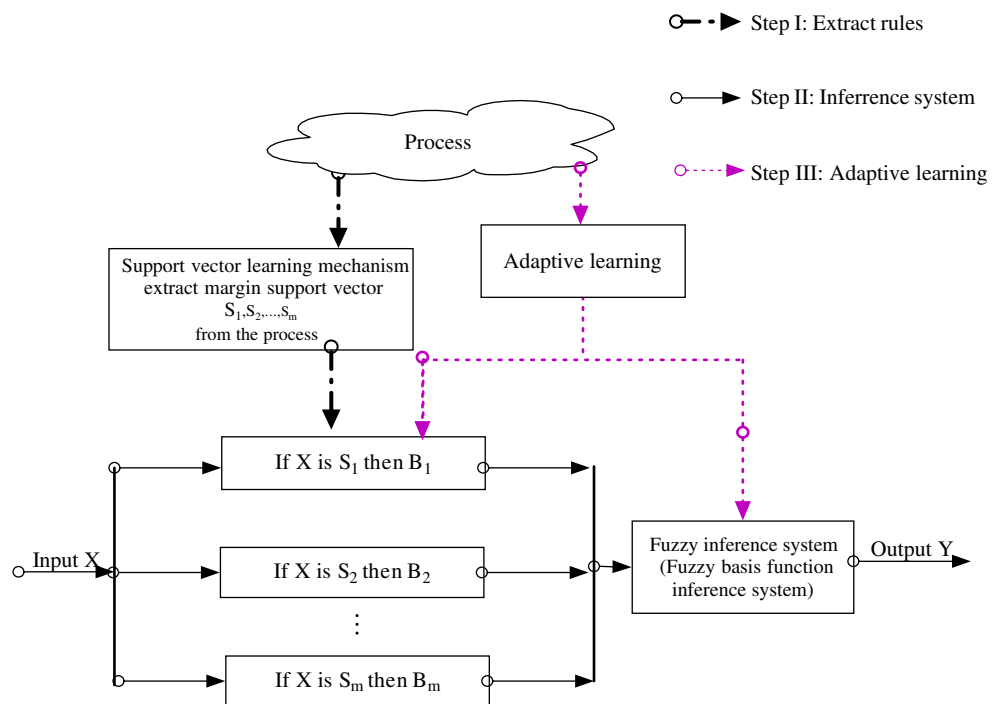
$$f(x) = \sum_{i=1}^l (\alpha_i - \alpha_i^*) K(x_i, x) + b. \tag{7}$$

An advantage of using the kernel function is that one can deal with the feature space of the arbitrary dimension without having to explicitly compute the map  $\varphi(x)$ . As such, any function that satisfies Mercer’s condition [13] can be used as a kernel function.

### 3 SVM-based fuzzy rules acquisition system with adaptive learning

In this section, we introduce a new fuzzy rule-based inference system utilizing SVM based on [8]. The architecture of the proposed SVM-based fuzzy inference is shown in Fig. 1. In this approach, the first step is to use SVM to extract the IF–THEN rules, then to adopt the fuzzy basis function inference system as the fuzzy inference system in the next step, and finally, to apply adaptive learning for the fuzzy rules and parameters in the fuzzy inference system. The main difference between SVM-FRAS and [8] is that the parameters in SVM-FRAS and fuzzy rules can be automatically tuned.

**Fig. 1** Schematic diagram of the SVM-based fuzzy rules acquisition system



### 3.1 Extract fuzzy rules using SVM

The SVM learning mechanism provides a solid foundation to extract the support vectors for further use in the generation of the IF–THEN rules. As described in the preceding section, only a minimal part of training data, particularly the support vectors, contribute to the solution. Geometrically, there are points that lie on or outside the  $\varepsilon$ -tube. In other words, they are in “key position”. It is important to note that we choose only the margin support vectors ( $0 < |\alpha_i - \alpha_i^*| < C$ ) because error support vectors ( $|\alpha_i - \alpha_i^*| = C$ ) may be far from the regression curve, as the empirical error should be equal or more than  $\varepsilon$  in this case.

### 3.2 Fuzzy inference system

We adopt the following fuzzy basis function inference system as the fuzzy inference system in this study:

$$y = f(x) = \sum_{j=1}^{N\_R} p_j(x)\bar{z}_j;$$

$$p_j(x) = \exp\left(-\sum_{k=1}^{N\_D} r_k \cdot (x_k - \bar{x}_{jk})^2\right) / \sum_{j=1}^{N\_R} \exp\left(-\sum_{k=1}^{N\_D} r_k \cdot (x_k - \bar{x}_{jk})^2\right) \tag{8}$$

where  $f:R^{N\_D} \rightarrow R$ ,  $N\_D$  is the number of the dimension of the input/output variables,  $N\_R$  is the number of rules,  $p_j(x)$  is the fuzzy basis function, which indicates how close the sample is to the  $j$ th rule,  $\bar{z}_j$  is the output of the  $j$ th rule,  $r_k$  is the coefficient of the  $k$ th dimension,  $x_k$  is the value of the  $k$ th dimension of the sample, and  $\bar{x}_{jk}$  is the value of the  $k$ th dimension of the  $j$ th rule.

Apparently, the most important advantage of using fuzzy basis functions is that an IF–THEN rule is directly related to a fuzzy basis function. Therefore, it provides a natural framework for combining both numerical and linguistic data in a uniform fashion. The inference system reflects the human habit of thinking: the closer the sample is to the rule, the closer the output of the sample is to the output of the rule.

### 3.3 Adaptive learning

In this section, we propose two adaptive learning methods for SVM-FRAS. The main focus is that the fuzzy rules are extracted by SVM directly from the samples, and although they are in key position, they do not exactly fit the fuzzy system. For this reason, it is important that the fuzzy rules and the fuzzy inference system should be tuned, so that the fuzzy system’s output could fit well the regression curve. To do such, we use the gradient methods to tune the output of the rule  $\bar{z}$  in the fuzzy rules and  $r_k$  in the fuzzy inference

system. The experiments show that in terms of accuracy, the adaptive learning methods exhibit excellent results.

#### 3.3.1 Adaptive batch learning algorithm

As the term implies, in batch algorithm, the input data are supplied in batch. The goal of adaptive learning is to minimize the total errors of the batch samples so we define the following error function:

$$E^* = \frac{1}{2} \sum_{l=1}^{N\_S} (y_l - y_{ld})^2 \tag{9}$$

where  $y_l$  is the output of the  $l$ th training sample,  $y_{ld}$  is the desired output, and  $N\_S$  is the number of samples.

The gradient method is used to solve the tuning problem for  $\bar{z}_j$ , the output of the  $j$ th rule:

$$\Delta\bar{z}_j = -\eta \frac{\partial E^*}{\partial \bar{z}_j} \tag{10}$$

where  $\eta$  is the learning rate.

Combining Eqs. 8, 9, and 10, we obtain the tuning formula for  $\bar{z}_j$ , where the output of the  $j$ th rule is

$$\Delta\bar{z}_j = -\eta \sum_{l=1}^{N\_S} (y_l - y_{ld}) \cdot p_j(x_l). \tag{11}$$

Using the gradient method to solve for the tuning approach for the coefficient of the  $k$ th dimension,  $r_k$ , we obtain the following:

$$\Delta r_k = -\eta \frac{\partial E^*}{\partial r_k} \tag{12}$$

Combining Eqs. 8, 9, and 12, we obtain the following:

$$\Delta r_k = -\eta \sum_{l=1}^{N\_S} (y_l - y_{ld}) \cdot \sum_{j=1}^{N\_R} \bar{z}_j \times \left( p_j(x_l) \left( -(x_{lk} - \bar{x}_{jk})^2 + \sum_{j=1}^{N\_R} (x_{lk} - \bar{x}_{jk})^2 \cdot p_j(x_l) \right) \right). \tag{13}$$

#### 3.3.2 Adaptive incremental learning algorithm

In incremental algorithm, the input data are supplied in sequence. The goal of adaptive learning is to minimize the training error of an incremental sample, and so we define the following error function:

$$E^* = \frac{1}{2} (y - y_d)^2 \tag{14}$$

where  $y$  is the output of the training sample and  $y_d$  is the desired output.

Moreover, the derivation is similar to the derivation in batch algorithm, so we give the update rule directly:

$$\Delta \bar{z}_i = -\eta(y - y_d)p_j(x) \tag{15}$$

$$\Delta r_k = -\eta(y - y_d) \sum_{j=1}^{N-R} \bar{z}_j \times \left( p_j(x) \cdot \left( -(x_k - \bar{x}_{jk})^2 + \sum_{j=1}^{N-R} (x_k - \bar{x}_{jk})^2 p_j(x) \right) \right). \tag{16}$$

### 4 SVM-FRAS-based adaptive inverse control

The architecture of the proposed SVM-FRAS-based adaptive inverse control is shown in Fig. 2. The control algorithm can be separated into two substages, namely, the identification stage and the control stage, where the (1) SVM-FRAS algorithm to train the system model was used and (2)  $u$  was obtained by using the SVM-FRAS inverse model to control output  $y$  according to reference input  $y_d$ .

#### 4.1 SVM-FRAS based identification

The mathematical model of the discrete-time nonlinear single-input single-output system can be described by Eq. 17:

$$y(k + 1) = f(y(k), \dots, y(k - n), u(k), \dots, u(k - m)) \tag{17}$$

where  $y \in R^n, u \in R^m, m \leq n, u$  and  $y$  represent the control input and output of the nonlinear system, respectively.

Define

$$X(i) = (y(i), y(i - 1), \dots, y(i - n), u(i), u(i - 1), \dots, u(i - m)) \tag{18}$$

where  $i=1,2,\dots,N$  refers to the number of samples. Equation 17 can be represented as

$$y(i + 1) = f(X(i)) \tag{19}$$

where  $f$  is the desired function. Constructing the learning sample  $(X(i), y(i + 1))$  and using the supporting vector

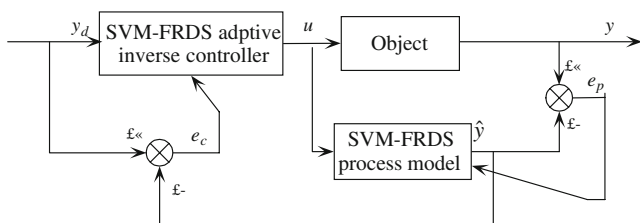


Fig. 2 Adaptive inverse control architecture based on SVM-FRAS

regression, the common form of fuzzy rules has been extracted:

$$R_j : \text{IF } X \text{ is } X(j), \text{ THEN } y \text{ is } y(j + 1)$$

where  $j=1, 2, \dots, N\_R, N\_R$  is the rule number,  $X$  is the input variable, and  $y$  is the output variable of the fuzzy system.

The model of  $y(k+1)$  is

$$y(k + 1) = \sum_{j=1}^{N-R} p_j(x) \cdot \bar{z}_j \tag{20}$$

$$p_j(x) = \exp \left( -r \|X(j) - X(k)\|^2 \right).$$

In this model,  $p_j(x)$  is the fuzzy basis function which measures the extent to which the sample approaches the  $j$  rule, and  $\bar{z}_j$  is the output of the  $R_j$  rule.

#### 4.2 SVM-FRAS-based inverse controller

Reference [14] is a detailed study on the invertible problem of Eq. 17. From such, the following conclusion is made:

*Theorem 1* If Eq. 17 is strictly monotone for  $u$ , the system is invertible at  $[y(k), \dots, y(k - n), u(k), \dots, u(k - m)]^T$ .

If the control process is revertible, then it is possible to construct the inverse model of the process using an appropriate method. This inverse model is the controller designed in this paper. Suppose that the system is invertible, then the inverse model of the system is the controller, that is,

$$u(k) = f^{-1}(y(k + 1), y(k), \dots, y(k - n), u(k - 1), \dots, u(k - m)) \tag{21}$$

where  $f^{-1}$  is the desired nonlinear function. As for the nonlinear system, it is difficult to obtain the analytical solution of the inverse model. However, since the process is invertible, there must exist an inverse model which may be estimated by the SVM-FRAS method.

Define

$$Y(k) = (y(k + 1), y(k), y(k - 1), \dots, y(k - n), u(i - 1), \dots, u(k - m)). \tag{22}$$

In constructing the learning sample  $(Y(i), u(i))$ , we extract the fuzzy rule model through the SVM-FRAS method:

$$R_j : \text{IF } Y \text{ is } Y(j), \text{ THEN } u \text{ is } u(j)$$

where  $j=1,2,\dots, N\_R, N\_R$  is the rule number,  $Y$  is the output variable, and  $u$  is the output variable of the fuzzy system.

The model of  $u(k)$  is

$$u(k) = \sum_{j=1}^{N-R} p_j(x) \cdot \bar{z}_j \tag{23}$$

$$p_j(x) = \exp \left( -r \|Y(j) - Y(k)\|^2 \right).$$

In this case,  $N\_R$  is the rules number, and  $p_j(x)$  is the fuzzy basis function which measures the extent to which the sample approaches the  $j$  rule.  $\bar{z}_j$  is the consequent of  $R$  rule. SVM-FRAS is applied to approximate the nonlinear function of  $f$  and  $f^{-1}$ . Furthermore, forward and inverse models are constructed, respectively. The accurate inverse model constructed by SVM-FRAS makes a steady-state gain between the controller and the model to be ranked 1. Thus, this guarantees no steady-state error in the tracking characteristic of the control system.

### 5 SVM-FRAS-based adaptive inverse control for the pulse GTAW process

#### 5.1 The technological parameters of welding and data collection

We use the experimental system of aluminum GTAW in [15]. Figure 3 shows the experiment system. The double-side visual sensor system captures the topside and backside images of the weld pool simultaneously. Aluminum alloy with 3 mm thickness is applied. With respect to the welding current, the scope is 160–230 A if it randomly changes every single sampling period. The scope is 165–215 A if it changes randomly every double sampling period. The wire feeding speed is 10 mm/s, and the welding speed is 3 mm/s. The parameters of welding technology are shown in Table 1. Accordingly, we collected 760 samples.

The schematic diagram of SVM-FRAS adaptive inverse control is shown in Fig. 4. The system consists of a

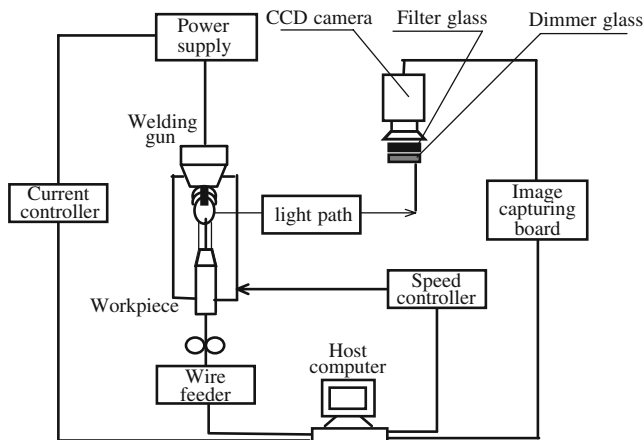


Fig. 3 The structure diagram of experimental system for GTAW

Table 1 Welding parameters of the AL alloy pulsed GTAW experiment

Welding joint	Closed flat butt joint	Peak value of the pulse current	Variable
Size of workpiece	250×50×4 mm	Peak current duration	250 ms
Base metal	Aluminum alloy LD 10	Base current duration	250 ms
Protective atmosphere	Argon gas (99.99%)	Diameter of tungsten electrode	4 mm
Welding current	Pulse alternating current	Arc length	4.5 mm
Current frequency	50 Hz	Welding speed	3 mm/s
Base value of the pulse current	90 A	Angle of tungsten electrode	85°

controlled object, process identification, a controller, and a sensor system of back weld width. The sensor system of backside weld width functions to predict backside weld width using key information on weld pool and weld parameters. System identification accomplishes the investigation of the forward model in the GTAW welding process through SVM-FRAS. The inverse model during the GTAW welding process constructed by SVM-FRAS constitutes the controller, where  $W_{bd}$  is the expected backside weld width,  $W_b$  is the backside weld width, that is, the output of the GTAW process,  $\hat{W}_b$  is the predicted back weld width of SVM-FRAS, that is, the model output of the GTAW process, and  $I$  is the peak current of pulse, which controls the input of the GTAW process.

#### 5.2 GTAW process model based on SVM-FRAS

From Eq. 17, the relation between backside weld width  $W_b$  and the peak current of pulse  $I$  could be obtained:

$$W_b(k + 1) = f(W_b(k), \dots, W_b(k - n), I(k), \dots, I(k - m)). \tag{24}$$

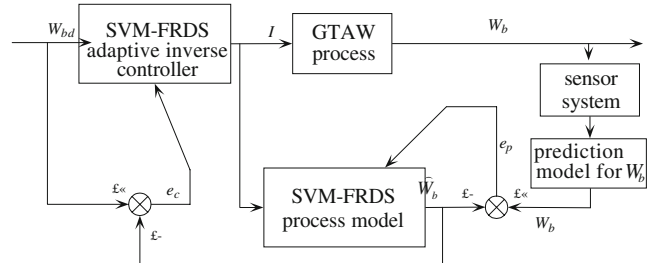


Fig. 4 Adaptive inverse control architecture for the GTAW welding process based on SVM-FRAS

**Table 2** Part rules extracted by SVM in the system identification for the pulsed GTAW process

I				O
$W_b(k)$	$W_b(k-1)$	$I(k)$	$I(k-1)$	$W_b(k+1)$
6.8	5.6	200	200	6.6
7.3	8.4	172	211	9
7.6	8.6	192	217	8
9.6	9.1	213	230	9.7
7.2	9.2	169	221	7.8
8.7	6.8	223	171	8.6

**Table 3** Part rules extracted by SVM in the controller for the pulsed GTAW process

I				O
$W_b(k+1)$	$W_b(k)$	$W_b(k-1)$	$I(k-1)$	$I(k)$
6.6	6.8	5.6	200	200
8	7.6	8.6	217	192
6.7	6.5	6.8	176	198
6.2	6.1	6.1	182	184
7.7	9.8	10.4	212	196
6.6	8.5	7.2	199	199
5.1	3.8	2	171	194

The parameters  $m, n$  should be identified in Eq. 24. Suppose  $m=n$  in consideration of the model precision and model complexity in the welding process. To investigate the influence of parameters  $m, n$  to the model, the data set is randomly split into 500 training samples and 260 test samples. The system identification of the GTAW process is initially made in the training set by SVM-FRAS. Moreover, the test in the above-mentioned model is made from the remaining 260 data. The testing method is used to compare the real value of the test sample and the output value of the model. When  $m, n \geq 1$  in the SVM-FRAS model, the root mean square (RMS) error of the system identification is 1 mm, meeting the requirement of process precision of welding and thus proving the validity of the SVM-FRAS-based method in the welding process' system identification. When  $m=n=2$ , the model will be much more precise. However, we set  $m=n=1$  in this experiment considering the aspect of model complexity.

The RBF kernel function  $K(x_i, x_j) = \exp(-\gamma \|x_i - x_j\|^2)$ ,  $\gamma > 0$  is applied for SVM-FRAS modeling in the welding

process. Using the obtained margin support vectors, we can derive a set of IF-THEN rules as Table 2.

The model of  $\bar{W}_b(k + 1)$  is:

$$\begin{aligned} \bar{W}_b(k + 1) &= \sum_{j=1}^{N_R} p_j(x) \cdot \bar{W}_{bj} \\ p_j(x) &= \exp(-r \|X(j) - X(k)\|^2) \\ X(i) &= (W_b(i), W_b(i - 1), I(i), I(i - 1)). \end{aligned} \tag{25}$$

Here,  $N_R$  is the number of rules which is about 50.  $p_j(x)$  is the fuzzy basis function which measures the extent to which the sample approaches the  $j$  rule.  $\bar{W}_{bj}$  is the result of the  $R_j$  rule.  $W_b(i)$  is the backside weld width at time  $i$ ;  $I(i)$  is the peak current at time  $i$ .

The prediction performance of the  $\bar{W}_b(k + 1)$  model is shown in Fig. 5. The identification of results shows that the SVM-FRAS model could better approximate the GTAW welding process.

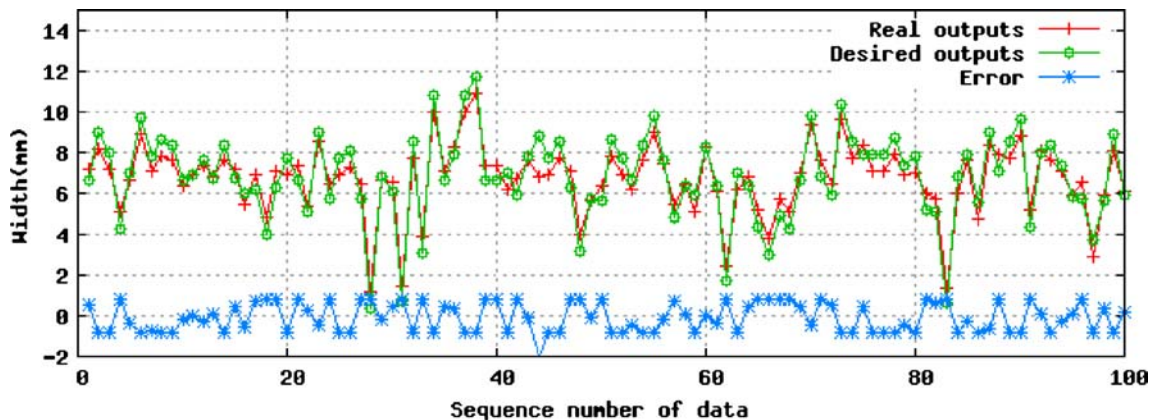


**Fig. 5** Identification results of the GTAW welding process using SVM-FRAS

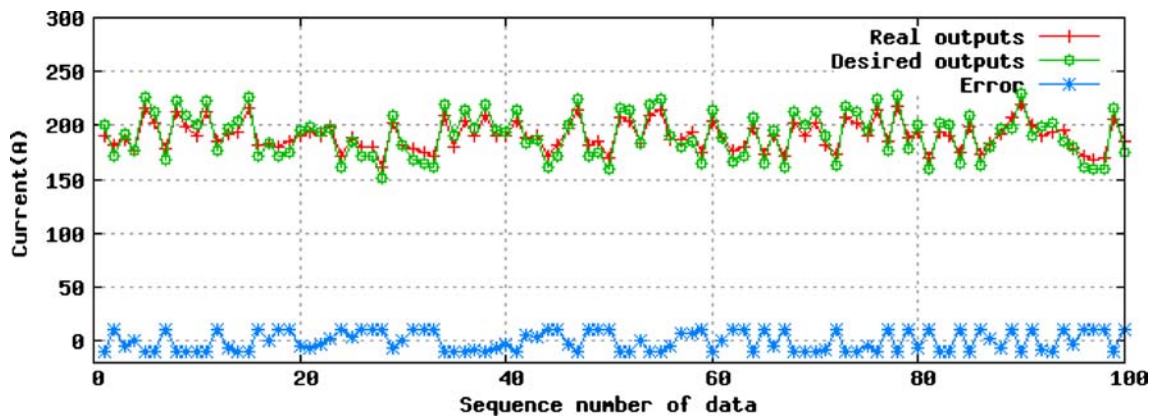


Fig. 6 Identification results of the GTAW welding process using the SVM-FRAS inverse model

### 5.3 Controller design based on SVM-FRAS

When  $m=n=1$ , the relation model between pulse peak current  $I$  and back weld width  $W_b$  is obtained from Eq. 21:

$$I(k) = f^{-1}(W_b(k + 1), W_b(k), W_b(k - 1), I(k - 1)). \tag{26}$$

In this study, the training set (500 data) and the test set (260 data) are randomly split to investigate the performance of the model. The controller design is first made in the training set using the SVM-FRAS inverse model. The rules set is obtained using margin support vectors through SVM, as shown in Table 3.

The reasoning model of the GTAW process controller is

$$I(k) = \sum_{j=1}^{N\_R} p_j(x) \cdot \bar{I}_j \tag{27}$$

$$p_j(x) = \exp\left(-r\|Y(j) - Y(k)\|^2\right)$$

$$Y(k) = (W_b(k + 1), W_b(k), W_b(k - 1), I(i - 1))$$

where  $N\_R$  is the number of rules, which is about 50. In addition,  $p_j(x)$  is the fuzzy basis function which measures the extent to which the sample approaches the  $j$  rule.  $\bar{I}_j$  is the result of the  $R_j$  rule,  $W_b(i)$  is the backside weld width at time, and  $I(i)$  is the peak current at time  $i$ .

A test is conducted using the remaining 260 test samples of the above-mentioned model. Comparison is as well made between the real values of the test sample and the output of the model in order to observe error changes. The identification precision of the SVM-FRAS inverse model, namely, the mean absolute error and RMS is 8.22 and 8.74 A, respectively. In Fig. 6, the identification result of the SVM-FRAS inverse model is shown. This further indicates the feasibility of making the SVM-FRAS inverse model as the controller of GTAW.

### 5.4 Simulation experiment of adaptive inverse control for the pulse GTAW welding process

In the simulation process, the backside weld width is calculated using the SVM-FRAS identification model, given that the welding process by the SVM-FRAS inverse controller could then be simulated. The initial welding condition is at the pulse peak current of  $I=185$  A, and the remaining parameters are all parameter values of the static model in the modeling process. Moreover, in the simulation process, the back weld width is set to 6 mm. Figure 7 shows the simulation result when  $W_b=6$  mm, and then from this simulation result, the maximum overshoot  $\delta_p$  is 3.3%. The regulating time is 3.5 s, and the steady-state error is 0.13 mm. The results obtained from the simulation show that SVM-FRAS inverse control can satisfy the requirements of the welding process.

## 6 Conclusion

A new method of adaptive inverse control based on the SVM-FRAS is proposed in this study. The proposed adaptive inverse control method can automatically extract control rule from the weld process data. Overall, the simulation experiments for the GTAW process show the efficacy of the SVM-FRAS adaptive inverse control method.

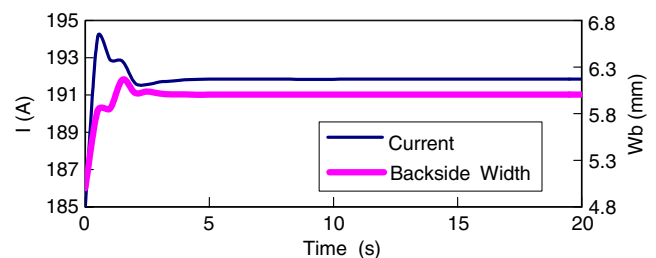


Fig. 7 The simulation curves of the adaptive inverse control architecture based on SVM-FRAS



**Acknowledgment** This work is supported by Shanghai Sciences & Technology Committee under grant no. 08DZ1202500 (08DZ1202502) and Young Faculty Research Grant of Shanghai Jiao Tong University.

## References

1. Chen SB, Lou YJ, Wu L, Zhao B (2000) Intelligent methodology for sensing, modeling, and control of pulsed GTAW: part 1-band-on-plate welding. *Weld J* 79:151–163
2. Chen SB, Zhao DB, Wu L, Lou YJ (2000) Intelligent methodology for sensing, modeling, and control of pulsed GTAW: part 2-but joint welding. *Weld J* 79:164–174
3. Chen SB, Wu L, Wang QL, Liu YC (1997) Self-learning fuzzy neural network and computer vision for control of pulsed GTAW. *Weld J* 76:201–209
4. Wang B, Chen SB, Wang JJ (2005) Rough set based knowledge modeling for the aluminum alloy pulsed GTAW process. *Int J Adv Manuf Technol* 25:902–908. doi:10.1007/s00170-003-1923-4
5. Li WH, Chen SB, Wang B (2008) A variable precision rough set based modeling method for pulsed GTAW. *Int J Adv Manuf Technol* 36:1072–1079. doi:10.1007/s00170-006-0922-7
6. Vapnik V (1995) *The nature of statistical learning theory*. Springer, New York, USA
7. Vapnik V (1998) *Statistical learning theory*. Wiley, New York
8. Huang XX, Chen SB (2006) SVM-based fuzzy modeling for the arc welding process. *Mater Sci Eng A Struct Mater Prop Microstruct Process* 427:181–187
9. Wang L, Mendel JM (1992) Fuzzy basis function, universal approximation, and orthogonal least-squares learning. *IEEE Trans Neural Netw* 3:807–814. doi:10.1109/72.159070
10. Smola AJ, Scholkopf B (2004) A tutorial on support vector regression. *Stat Comput* 14:199–222. doi:10.1023/B:STCO.0000035301.49549.88
11. Karush W (1939) *Minima of functions of several variables with inequalities as side constraints*. Master's thesis, Department of Mathematics, University of Chicago, Chicago
12. Kuhn HW, Tucker AW (1951) *Nonlinear programming*. Proc. 2th Berkeley Symp. Mathematical Statistics and Probabilities. University of California Press, Berkeley
13. Courant R, Hilbert D (1953) *Methods of mathematical physics*. Wiley, New York
14. Widrow B, Walach EW (1996) *Adaptive inverse control*. Prentice-Hall, New Jersey
15. Fan CJ, Wang JJ, Chen SB (2007) Visual sensing and image processing in aluminum alloy welding. *Lect Notes Contr Inf Sci* 362:275–280. doi:10.1007/978-3-540-73374-4\_32